

Original Research

A novel multiple subdivision-based algorithm for quantitative assessment of retinal vascular tortuosity

Gengyuan Wang^{1,*} , Meng Li^{1,*} , Zhaoqiang Yun² , Zhengyu Duan¹, Ke Ma¹, Zhongzhou Luo¹, Peng Xiao¹  and Jin Yuan¹

¹State Key Laboratory of Ophthalmology, Zhongshan Ophthalmic Center, Sun Yat-sen University, Guangzhou 510060, China; ²School of Biomedical Engineering, Southern Medical University, Guangzhou 510515, China

Corresponding authors: Peng Xiao. Email: xiaopengaddis@hotmail.com; Jin Yuan. Email: yuanjincomea@126.com

*These authors contributed equally to this work.

Impact statement

Since the vascular tortuosity of retinal vessels has been proven to be an early indicator for the early diagnosis, various quantification methods have been proposed but can be hardly applied into clinical application due to low consistency with experts' assessment. We reported here a quantitative vascular tortuosity analysis algorithm based on multiple subdivision of vessel segments incorporating a learning curve function of the curve bending number. Our results showed high correlation with experts' prediction in vascular tortuosity of retinal fundus images, demonstrating that the proposed method shows promise for automatic and objective vascular tortuosity evaluation of retinal fundus images in clinical applications.

Abstract

Vascular tortuosity as an indicator of retinal vascular morphological changes can be quantitatively analyzed and used as a biomarker for the early diagnosis of relevant disease such as diabetes. While various methods have been proposed to evaluate retinal vascular tortuosity, the main obstacle limiting their clinical application is the poor consistency compared with the experts' evaluation. In this research, we proposed to apply a multiple subdivision-based algorithm for the vessel segment vascular tortuosity analysis combining with a learning curve function of vessel curvature inflection point number, emphasizing the human assessment nature focusing not only global but also on local vascular features. Our algorithm achieved high correlation coefficients of 0.931 for arteries and 0.925 for veins compared with clinical grading of extracted retinal vessels. For the prognostic performance against experts' prediction in retinal fundus images from diabetic patients, the area under the receiver operating characteristic curve reached 0.968, indicating a good consistency with experts' predication in full retinal vascular network evaluation.

Keywords: Fundus photography, vascular tortuosity, multiple subdivision

Experimental Biology and Medicine 2021; 246: 2222–2229. DOI: 10.1177/15353702211032898

Introduction

The retina is one of the few tissues throughout the body where blood vessels can be non-invasively observed *in vivo* with photographic techniques like fundus photography or optical coherence angiography (OCTA), providing cost-efficient and highly repeatable access for studying the microcirculation and the hemodynamic of blood flow.^{1,2} Retinal vessels are thought to reflect the general status of the microvasculature in human body as the eye itself is one of the target organs affected by vascular diseases.³ Analyzing the vascular system in the eye fundus can resolve common symptoms including neovascularization, occurrence of pathological structures, or vascular morphological alteration.⁴ To perform quantitative evaluation of

retinal vascular system, various studies have been conducted to extract vessel morphological parameters including vessel diameter, density, branching, tortuosity, etc. and assess their relationship with systemic and ocular diseases.^{5,6}

Since the early diagnosis and effective treatment are important to most of the diseases, retinal vascular tortuosity variation has been identified as one of earliest indicators to a number of relevant diseases such as diabetes, cerebrovascular disease, stroke, and ischemic heart disease.^{4,7} Vascular tortuosity is defined by the degree of being tortuous of blood vessels (curved and twisted, having many turns). While it is crucial to ensure repeatable and reliable evaluation of vascular tortuosity, it is difficult to

describe and annotate with words due to the lack of a precise and standardized protocol and its manual evaluation is often tedious and introduces a high inter and intra operator variability.^{8,9} Thus, automatic and precise quantification of retinal vascular tortuosity is of great significance.

To quantify retinal vascular tortuosity, various numbers of computational approaches have been proposed and applied,¹⁰⁻²³ mostly based on retinal fundus images as it is the most widely accessible retinal imaging method. One common vascular tortuosity measurement method introduced by Hart *et al.* is calculating the ratio of the length to the chord of blood vessel segment centrelines,¹³ based on which some other length-based calculations have also been developed and applied to clinical studies in subsequent researches.¹⁴⁻¹⁶ Hart *et al.* also applied the concept of total curvature,¹⁷ which was later introduced with changes by Bhuiyan *et al.* considering numerical derivative for the calculus of the total curvature¹⁸ and Trucco *et al.* generalizing the vessel skeleton curvature measurement.¹⁹ Other changes like average angular transformation and integral of curvature squared have also been introduced for the curvature-based calculation of retinal vascular tortuosity.²⁰

Nevertheless, most of the computational retinal vascular tortuosity measurement methods tend to evaluate the vascular tortuosity in a relatively global way while failed to evaluate the actual turns and twists within the vessel segment.²¹⁻²³ Moreover, since the retinal vascular tortuosity evaluation in clinical practice is mostly based on the experts' experience, computational methods do not always match the clinical concept of tortuosity.²⁴ In order to perform better quantitative retinal vascular evaluation with improved mathematical metrics while being robust enough to compare with those perceived by ophthalmologists: Grisan *et al.* proposed an approach based on partitioning each vessel segment into sub-segments of constant-sign curvature and combining together each calculation;²⁵ Onkaew *et al.* developed an alternative method by using the curvature calculated from improved chain code algorithm taking the number of inflection point of a vessel segment into account;²⁶ Ramos *et al.* proposed a novel computational tortuosity assessment incorporating clinically domain-related anatomical information, providing more adjusted evaluation to the specialists' perception.²⁷

In this study, in order to be more in line with manual assessment, we demonstrated a novel retinal vascular tortuosity quantification method based on multiple subdivision of retinal vessels. With automatic retinal vessel network segmented and split into single vessel segments, multiple subdivision algorithm is applied to divide single vessel into overlapping sub-segments corresponding to the continuous changing chord lengths. The tortuosity index of a single vessel segment is calculated as the maximum of the accumulated absolute tangent angle difference of the sub-segments multiplied by a transformed sigmoid learning curve function of the inflection point numbers of the vessel segment curvature sign, giving prominence to local vascular turns and twists. The performance of our newly

defined vascular tortuosity measurement algorithm was compared with traditional arc length to chord length ratio method introduced by Hart *et al.*¹³ and tortuosity evaluation method developed by Grisan *et al.*²⁵ in analyzing the RET-TORT public data of retinal vessels. Tortuosity analysis and prognostic performance against expert observers' evaluation were also demonstrated on a clinical fundus image dataset of diabetic patients.

Materials and methods

Dataset

Considering the relation between retinal vascular tortuosity and diabetes,^{14,28,29} in this study, we included 104 retinal fundus images of diabetic patients ranging from non-visible vascular abnormality to severe vascular tortuosity without other obvious pathological structures like exudates, hemorrhages, microaneurysms, etc. The fundus images were taken by a fundus camera (Topcon, TRC-50DX, Japan) with 50° field of view. All the data used have been anonymized. The experimental procedures adhered to the tenets of the Declaration of Helsinki [1983] and were approved by the Institutional Review Board of Zhongshan Ophthalmic Centre, Sun Yat-sen University, China (protocol number: 2017KYPJ104). Three mid-level or higher ophthalmologists actively involved in daily clinical practice were asked to give their perspectives in three different rounds regarding whether the retinal vascular network is tortuous or not. While there is no standard guide for retinal tortuosity evaluation presented, for manual evaluation of the retinal vascular tortuosity, ophthalmologists typically integrate the information on how many times a vessel turns and twists and how large the amplitude turning amplitude is based on their daily clinical experience. Note that, in retinal fundus image, straight vessels typically present a smooth semi-circular or parabolic shape due to the hemispherical shape of the retina. The rating scale is defined as zero for negative and one for positive, respectively. To establish a unified criteria for the characterization of quantitative retinal vascular tortuosity assessments, the result for each ophthalmologist is marked as their own opinion being consistent for more than twice on every fundus image, and the final ground truth for the dataset is formed by the same opinion of more than two ophthalmologists.

Vessel segmentation

Before performing computational retinal vascular tortuosity analysis, the first step is to segment the vascular network from the retinal fundus image and extract the vessel segments as shown in Figure 1. For vessel network and optic disc segmentation, a multi-path recurrent U-Net network architecture combining a convolutional neural network and a recurrent neural network is used.³⁰ In this algorithm, the applied multi-branching of the encoding path and the decoding path ensure more effective semantic features extraction, and the multi-path recurrent U-Net combines the recurrent neural network further improves the target features by sequencing the multi-path output features in

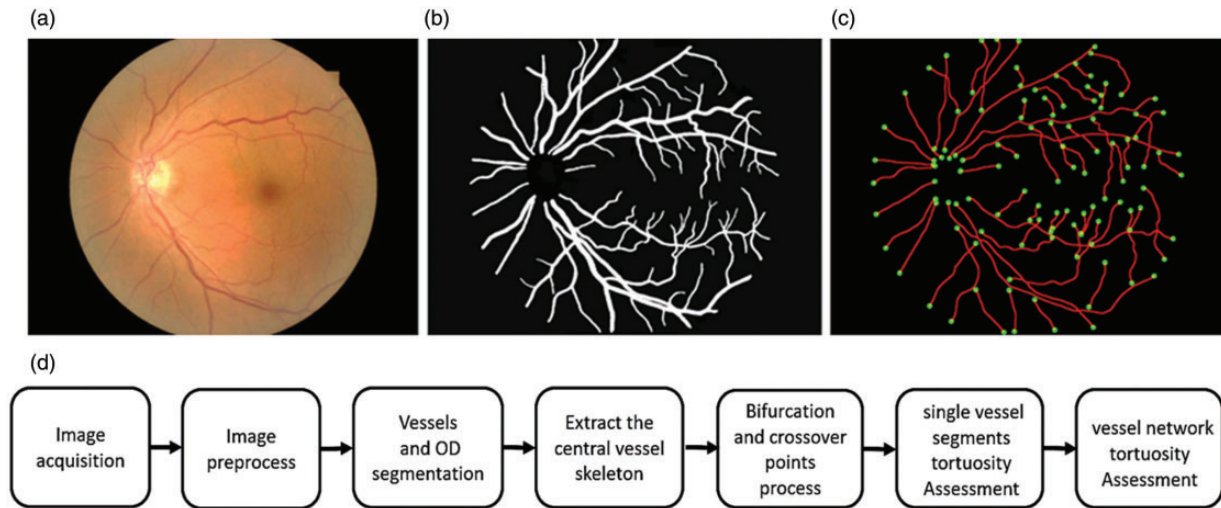


Figure 1. Vessel segmentation process and flow chart depicting steps for retinal vessels tortuosity assessment. (a) The original fundus image, (b) the segmented retinal vascular network, (c) the extracted single vessel segments readily for tortuosity evaluation, and (d) flow chart depicting steps for vascular tortuosity assessment. (A color version of this figure is available in the online journal.)

time, thus ensuring more accurate retinal vessel and optic disc segmentation. The original retinal fundus image of 2656×1992 pixels is firstly rescaled to 512×512 pixels before feeding into the network. With the retinal vascular network and the optic disc segmented, the optic disc area is subtracted from segmented vascular network to remove the twisted overlapping optic disc vessels that may interfere future tortuosity analysis. Then the resulted prediction image is padded to the original image size obtaining binary vascular network image (Figure 1(b)). A thinning process with fast parallel algorithm³¹ is further applied to the binary vascular networks to extract the central vessel skeleton. Finally, based on the geometrical and topological properties of the blood vessels, bifurcation and crossover points of the vessels are detected and eradicated at vessel skeleton centerline pixels with more than two neighbors, reconnected for crossover vessels and branches with similar vessel diameter,³² splitting the skeletonized vascular network into single vessel segments readily for tortuosity evaluation (Figure 1(c)).

Multiple subdivision-based vascular tortuosity assessment

The common mathematical model proposed by Hart *et al.* for measuring vascular tortuosity is defined by the ratio of the length of the curve to the chord length

$$\tau_h = \frac{L_c}{L_a} - 1 \quad (1)$$

where L_c is the length of the curve, calculated by all the points from the beginning to the end of a vessel segment, and L_a is the length of the underlying chord, which is actually the Euclidean distance between the starting and ending points of a vessel segment. However, this method is insufficient to reflect the small variations of vessel segments. To address the number of twists and local winding, Grisan

et al. proposed modifications by subdividing each vessel segment into sub-segments of constant-sign curvature and combining them together for global evaluation as follows

$$\tau_g = \frac{n-1}{n} \cdot \frac{1}{L_c} \sum_{i=1}^n \left[\frac{L_{ci}}{L_{ai}} - 1 \right] \quad (2)$$

where L_c is the length of vessel segment, L_{ci} and L_{ai} represent the arc length and chord length of sub-segment i , and n is the total number of sub-segments. Nevertheless, the main drawbacks are its scale dependency and it is indistinguishable for curves with only one curvature changing point.²⁵

To better match manual evaluation concept of vascular tortuosity focusing not only global but also various local features while being scale independent, based on the concept of multiple subdivision that has been widely applied to fractal patterns,^{33,34} we propose a multiple subdivision-based method for vessel tortuosity index analysis by sequentially splitting single vessel segment into overlapping sub-segments with continuous increasing equal chord length and calculate the accumulated absolute tangent angle difference of sub-segments corresponding to different chord lengths. The detailed concept is illustrated in Figure 2. For the first division, with minimum unit chord length ($\Delta L_A = 1 \text{ pixel}$), a single vessel is subdivided into k_1 parts (Figure 2(a)). The split points of the sub-segments of the first division are marked as p_0, p_1, \dots, p_{k1} . For the second division, segmentation is performed sequentially from each split point (p_0, p_1, \dots, p_{k2}) with chord length of $2\Delta L_A$, until the left segment chord length is less than $2\Delta L_A$, extracting k_2 vessel sub-segments (Figure 2(b)). By this analogy, for the subsequent n^{th} division, k_n sub-segments of the vessel are extracted starting from split points (p_0, p_1, \dots, p_{kn}) with multiple unit chord length of $n\Delta L_A$, until the single vessel segment chord length is smaller

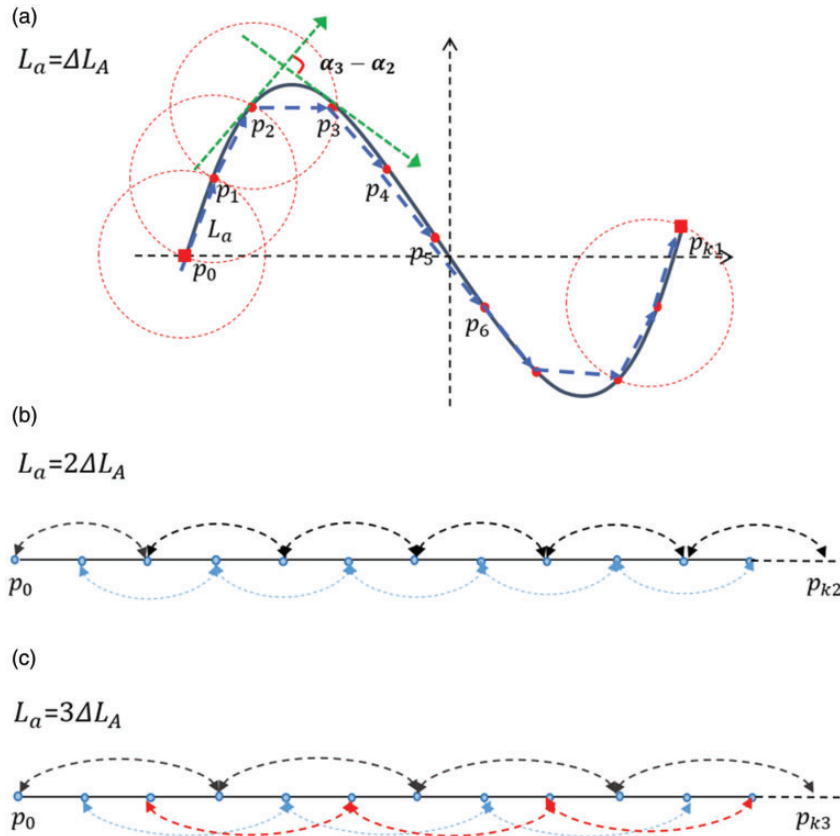


Figure 2. Schematic demonstrating the principle of multiple subdivision method for the overlapping split of extracted vessel segment for vascular tortuosity computation. (a) For the first division, the curve is continuously subdivided with fixed chord length $L_a = \Delta L_A$, and the accumulated absolute tangent angle differences of the split sub-segments' endpoints are calculated. (b) The second division is performed with fixed chord length $L_a = 2\Delta L_A$ at each split point of the first division with the sub-segments overlapped with each other. (c) The third division is performed with fixed chord length $L_a = 3\Delta L_A$ at each split point of the first division. (A color version of this figure is available in the online journal.)

than $n\Delta L_A$. To analyze the vascular tortuosity, the accumulated absolute tangent angle difference $\phi(n)$ of all the corresponding sub-segments of each division n is calculated, and the maximum value Φ of the accumulated absolute tangent angle difference is extracted.

$$\Phi = \max(\phi(n)) = \max\left(\sum_{i=1}^{k_n} \alpha_{i-1} - \alpha_i\right) \quad (3)$$

where n is the sequence number of the multiple division, k_n is the corresponding numbers of vessel sub-segments, α_{i-1} and α_i are the tangent angle values at the endpoints of the i^{th} sub-segment in the n^{th} division. Note that for n^{th} division, $1 \leq k_n \leq k_1$.

Considering that the number of local turns and twists of a vessel play an important role in matching the computational tortuosity evaluation to the manual concept as Grisan *et al.* described,²⁵ a learning curve model represented by a modified logistic function^{35,36} of the inflection point numbers of the vessel segment curvature sign is further introduced into the tortuosity index calculation, incorporating the artificial evaluation nature of fast and rapid tortuosity increase with the increase of curvature inflection point numbers but trends to reach a limit when the number is

too large. The final tortuosity index τ of a single vessel segment is defined as

$$\tau = \frac{1}{1 + e^{-\frac{1}{2}(m-4)}} \cdot \Phi \quad (4)$$

where m is the number of the inflection points at which the second derivative of vessel segment centerlines vanishes, and is identified by detecting changes in the sign of curvature³⁷

$$C = \frac{\Delta\alpha}{\Delta s} \quad (5)$$

where Δs is the arc length that is greater than 0. The sign change of curvature C depends on the difference of the tangent angle $\Delta\alpha$ between adjacent split points. The coefficients of the logistic function in tortuosity index are selected to optimize the correlation between our computational tortuosity index and the human observer results on the evaluation of vascular tortuosity as shown in the latter validation part of the paper. To quantify a retinal fundus image, its global tortuosity index $\bar{\tau}$ is calculated as the averaged tortuosity indices of all the single vessel segments from the extracted vessel network.

Validation and experiments

To validate the performance of our newly defined multiple subdivision-based vascular tortuosity algorithm, a publicly available dataset of retinal vessels with clinical annotations of vascular tortuosity, RET-TORT,²⁵ is used. Established by the University of Padova, RET-TORT contains extracted retinal vessel images of 30 arteries and 30 veins, which are ranked independently by their tortuosity. With our automatic tortuosity analysis method, the tortuosity indices τ of all the arteries and veins are calculated. The performance of our algorithm is demonstrated using Spearman's rank correlation with SPSS (SPSS Inc., SPSS Statistics V25, USA) between the automatic results and the clinical annotations of the vascular tortuosity. Statistical significance was set at $P \leq 0.05$. The correlation coefficient of the multiple subdivision-based vascular tortuosity index τ is also compared with those of the traditional vascular tortuosity τ_h introduced by Hart *et al.* (formula (1)) and the previous established tortuosity index τ_g developed by Grisan *et al.* (formula (2)).

Since the assessment of the whole retinal vascular network tortuosity is important for the clinical need in aiding

Table 1. Spearman's rank correlation coefficients of the tortuosity indices (τ , τ_h , τ_g) with the clinical grading for the RET-TORT dataset.

Tortuosity measure	Correlation coefficient	
	Arteries	Veins
τ_h^{25}	0.792	0.656
τ_g^{25}	0.949	0.853
T	0.931	0.925

diagnosis, tortuosity analysis and its prognostic performance evaluation are performed on our own clinical fundus image dataset. With the ground truth of whether the retinal fundus images are tortuous or not defined by the ophthalmologists, all the 104 included fundus image are processed by the aforementioned algorithm, acquiring their global tortuosity indices $\bar{\tau}$. To evaluate the prognostic performance of our multiple subdivision-based tortuosity index against the experts' prediction, the association between $\bar{\tau}$ and clinical experts' grading ground truth is established using Spearman's rank correlation with SPSS (SPSS Inc., SPSS Statistics V25, USA), statistical significance was accepted at $P \leq 0.05$. An ROC (Receiver Operating Characteristic) analysis is also performed by using the tortuous/non-tortuous classification as the target ground truth. Thus, the ROC curve can be built from the reciprocal relation between sensitivity and specificity calculated for all the possible threshold values for the calculated tortuosity index $\bar{\tau}$.³⁸ The ROC analysis is also conducted in SPSS (SPSS Inc., SPSS Statistics V25, USA).

Results

Validation results

Table 1 shows the Spearman's rank correlation coefficients results from the correlation of our tortuosity index τ with the clinician's grading for the 30 arteries and 30 veins in the RET-TORT. The correlation coefficients for tortuosity indices τ_h and τ_g are also shown in Table 1 for comparison.²⁵ Our multiple subdivision-based tortuosity index τ has achieved a high correlation coefficients of 0.931 for arteries and 0.925 for veins in the RET-TORT, indicating better

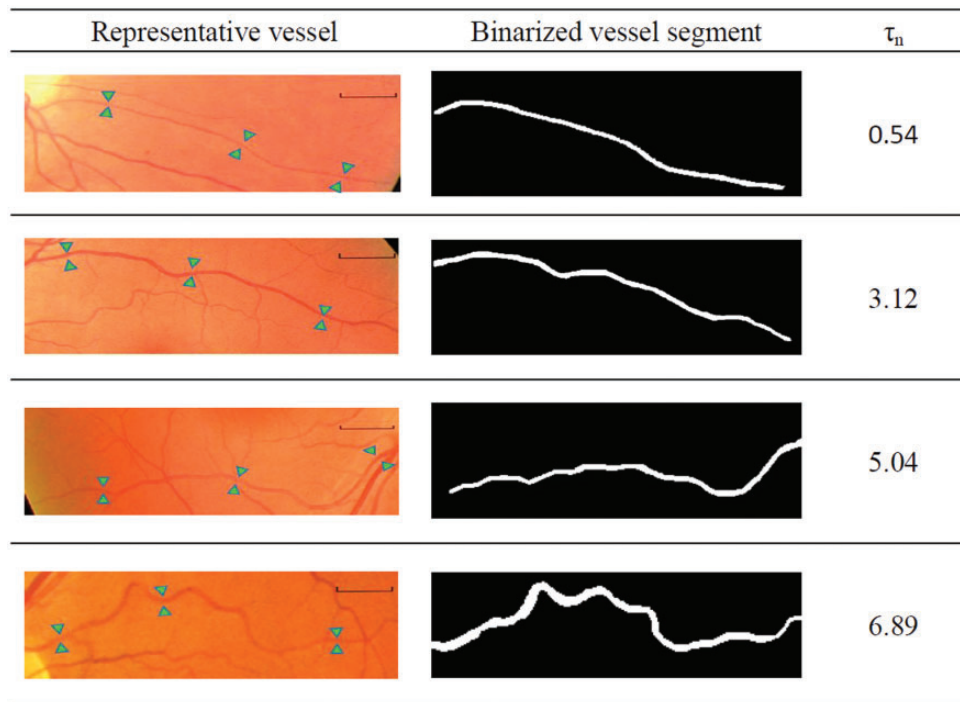


Figure 3. Vascular tortuosity index τ of representative vessels extracted from fundus images. The extracted fundus images of vessels are shown in the left column, the corresponding binarized single vessel segments are shown in the middle column. The tortuosity indices τ of the single vessels are displayed in the right column. Scale bar: 300 μm . (A color version of this figure is available in the online journal.)

while balanced correlation with experts' evaluation in vascular tortuosity. Though our correlation coefficient for arteries is a little bit lower than τ_g , we have much better correlation results for the veins.

Representative vessels extracted from retinal fundus images (Figure 3, left column) and vascular tortuosity analysis results are shown in Figure 3, demonstrating the correspondence of the vessel morphology to the newly defined vascular tortuosity index. As the results show, the larger degree of the vascular curving and the more local turns and twists, the higher the tortuosity index τ .

Full fundus image analysis results

Figure 4 shows the global tortuosity analysis results of three representative fundus images. The original fundus images are shown in the left column, and the corresponding segmented vessel network are shown in the middle column. The global tortuosity indices $\bar{\tau}$ of the images are displayed in the right column. For fundus image with obvious tortuous vascular network, the global vascular tortuosity index is much larger.

The Spearman's rank correlation coefficient between the global tortuosity indices $\bar{\tau}$ and clinical experts' grading ground truth reaches 0.82. Figure 5 shows the ROC curve of the global tortuosity index $\bar{\tau}$ for the vascular network tortuosity classification against the ground truth defined by experts' prediction. The prognostic performance accuracy of our multiple subdivision-based global tortuosity index $\bar{\tau}$ evaluated by calculating the area under the ROC curve (AUC) is 0.968, indicating a high prognostic performance.

Discussion

In this study, we reported a multiple subdivision-based algorithm for the vascular tortuosity analysis of retinal fundus images. Our algorithm showed good correlation (0.931 for arteries and 0.925 for veins) with experts' grading of vascular tortuosity in extracted retinal vessels. The prognostic performance of the algorithm against experts' prediction in evaluating vascular tortuosity of full retinal fundus images achieved a high AUC of 0.968.

Compared with the pre-published retinal vascular tortuosity methods either considering single vessel segment as

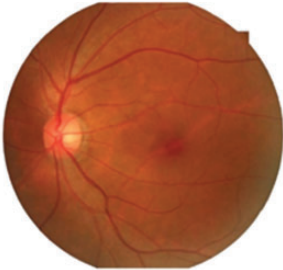



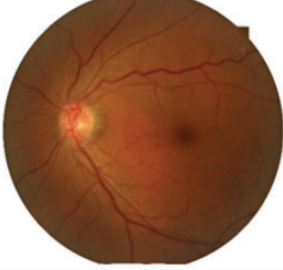

Fundus image	Vascular network	Global tortuosity index $\bar{\tau}$
		0.51±0.04
		2.57±0.12
		4.33±0.16

Figure 4. Global vascular tortuosity index $\bar{\tau}$ of representative fundus images. The original fundus images are shown in the left column, the corresponding segmented vessel network is shown in the middle column. The acquired global tortuosity indices $\bar{\tau}$ of the images are displayed in the right column. (A color version of this figure is available in the online journal.)

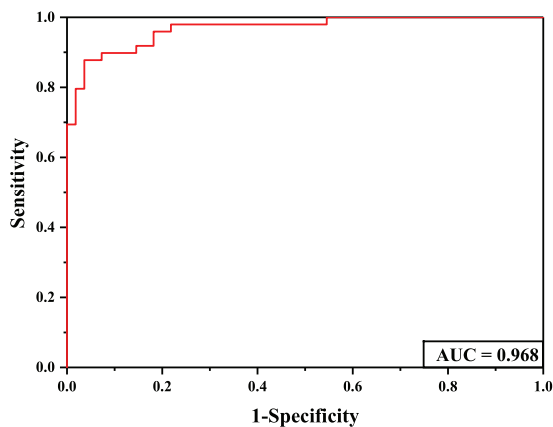


Figure 5. Prognostic performance demonstrated by ROC curve of the global tortuosity index $\bar{\tau}$ for the vascular network tortuosity classification against the ground truth defined by experts' prediction. AUC: the area under the ROC curve. (A color version of this figure is available in the online journal.)

a whole or dividing into fixed sub-segments, we introduced for the first time the concept of multiple subdivision into vascular tortuosity analysis by splitting vessel segment with continuous changing chord length into overlapping sub-segments, being more in line with human assessment considering not only global but also focusing on local vascular features within various vision field scale. Moreover, a learning curve function of the inflection point numbers of the vessel segment curvature sign was also incorporated mimicking the visual perception of fast vascular tortuosity increase with the number of local turns but trend to reach a rooftop in the end. Although the correlation coefficient with the clinician's grading of our algorithm in the arteries tortuosity analysis is slightly lower than Grisan *et al.* (0.931 for τ and 0.949 for τ_g), we have a much better correlation coefficient in the evaluation of the veins (0.925 for τ and 0.853 for τ_g), achieving the highest averaging correlation coefficient in processing the same dataset compared with the pre-published methods described in Table 1 in Grisan *et al.*²⁵ In the prognostic performance evaluation against experts' evaluation on the vascular tortuosity of full retinal fundus images taken from diabetic patients, our algorithm also showed a higher AUC (0.968) compared with the methods developed by Hart *et al.* (0.66),¹⁷ Trucco *et al.* (0.65),¹⁹ Grisan *et al.* (0.80),²⁵ and Onkaew *et al.* (0.72)²⁶ as demonstrated in Figure 4 in Ramos *et al.*²⁷ While our algorithm is proposed for the vascular tortuosity analysis of retinal fundus images, it can also be applied to OCTA images if the vascular network segmented properly. Nevertheless, the main challenge would remain on the proper vessel segmentation since OCTA images contains massive and dense capillaries.³⁷

Conclusions

In conclusion, our multiple subdivision-based algorithm has achieved a good performance in evaluating the vascular tortuosity of retinal fundus images. Since previous studies have shown differences in the degree of twisting between arteries and veins,^{39,40} future work focusing on the measurement of vascular tortuosity on the basis of

retinal arterial and venous classification would provide richer information for the evaluation of retinal fundus images.

AUTHORS' CONTRIBUTIONS

Conceptualization, GW, PX, and JY; Investigation and Data Collection, ML, ZL and ZD; Methodology, GW, KM and PX; Software, GW; Writing - original draft, GW, PX; Writing - review and editing, GW, ML, ZD, KM, PX and JY; Supervision, PX and JY.

DECLARATION OF CONFLICTING INTERESTS

The author(s) declared no potential conflicts of interest with respect to the research, authorship, and/or publication of this article.





FUNDING

The author(s) disclosed receipt of the following financial support for the research, authorship, and/or publication of this article: This research was supported by the grant from the Key-Area Research and Development Program of Guangdong Province (2019B010152001) and the National Natural Science Foundation of China (81870633, 81901788).

DATA AVAILABILITY

The data used to support the findings of this study are available from the first author upon request.

ORCID IDS

Gengyuan Wang  <https://orcid.org/0000-0002-7416-3975>
Meng Li  <https://orcid.org/0000-0001-6656-8713>
Zhaoqiang Yun  <https://orcid.org/0000-0002-6367-4403>
Peng Xiao  <https://orcid.org/0000-0002-2860-0249>

REFERENCES

- Taylor HR, Keeffe JE. World blindness: a 21st century perspective. *Br J Ophthalmol* 2001;**85**:261-6
- Nagiel A, Satta SVR, Sarraf D. A promising future for optical coherence tomography angiography. *JAMA Ophthalmol* 2015;**133**:629-30
- Stanton AV, Wasan B, Cerutti A, Ford S, Marsh R, Sever PP, Hughes AD. Vascular network changes in the retina with age and hypertension. *J Hypertens* 1995;**13**:1724-8
- Koreen S, Gelman R, Martinez-Perez ME, Jiang L, Berrocal AM, Hess DJ, Chiang MF. Evaluation of a computer-based system for plus disease diagnosis in retinopathy of prematurity. *Ophthalmology* 2007;**114**:e59-e67
- Cheung CY, Tay WT, Ikram MK, Ong YT, De Silva DA, Chow KY, Wong TY. Retinal microvascular changes and risk of stroke: the Singapore Malay Eye Study. *Stroke* 2013;**44**:2402-8
- Nguyen TT, Wang JJ, Wong TY. Retinal vascular changes in pre-diabetes and prehypertension: new findings and their research and clinical implications. *Diabetes Care* 2007;**30**:2708-15
- Heitmar R, Lip GYH, Ryder RE, Blann AD. Retinal vessel diameters and reactivity in diabetes mellitus and/or cardiovascular disease. *Cardiovasc Diabetol* 2017;**16**:10
- Benitez-Aguirre P, Craig ME, Sasongko MB, Jenkins AJ, Wong TY, Wang JJ, Donaghue KC. Retinal vascular geometry predicts incident retinopathy in young people with type 1 diabetes: a prospective cohort study from adolescence. *Diabetes Care* 2011;**34**:1622-7

9. Crosby-Nwaobi R, Heng LZ, Sivaprasad S. Retinal vascular calibre, geometry and progression of diabetic retinopathy in type 2 diabetes mellitus. *Ophthalmologica* 2012;**228**:84–92
10. Capowski JJ, Kylstra JA, Freedman SF. A numeric index based on spatial frequency for the tortuosity of retinal vessels and its application to plus disease in retinopathy of prematurity. *Retina* 1995;**15**:490–500
11. Wallace DK. Computer-assisted quantification of vascular tortuosity in retinopathy of prematurity (an american ophthalmological society thesis). *Trans Am Ophthalmol Soc* 2007;**105**:594–615
12. Bullitt E, Gerig G, Pizer SM, Lin W, Aylward SR. Measuring tortuosity of the intracerebral vasculature from MRA images. *IEEE Trans Med Imaging* 2003;**22**:1163–71
13. Hart WE, Goldbaum M, Côté B, Kube P, Nelson MR. Measurement and classification of retinal vascular tortuosity. *Int J Med Inform* 1999;**53**:239–52
14. Sasongko MB, Wong TY, Nguyen TT, Cheung CY, Shaw JE, Wang JJ. Retinal vascular tortuosity in persons with diabetes and diabetic retinopathy. *Diabetologia* 2011;**54**:2409–16
15. Martinez-Perez ME, Hughes AD, Stanton AV, Thorn SA, Chapman N, Bharath AA, Parker KH. Retinal vascular tree morphology: a semi-automatic quantification. *IEEE Trans Biomed Eng* 2002;**49**:912–7
16. Goh KG, Hsu WL, Lee M, Wang H. ADRIS: an automatic diabetic retinal image screening system. *Stud Fuzziness Soft Comput* 2001;**60**:181–210
17. Hart WE, Goldbaum M, Cote B, Kube P, Nelson MR. Automated measurement of retinal vascular tortuosity. *Proc AMIA Annu Fall Symp* 1997;459–63
18. Bhuiyan A, Nath B, Ramamohanarao K, Kawasaki R, Wong TY. Automated analysis of retinal vascular tortuosity on color retinal images. *J Med Syst* 2012;**36**:689–97
19. Trucco E, Azegrouz H, Dhillon B. Modeling the tortuosity of retinal vessels: does caliber play a role? *IEEE Trans Biomed Eng* 2010;**57**:2239–47
20. Hughes AD, Martinez-Perez E, Jabbar AS, Hassan A, Witt NW, Mistry PD, Chapman N, Stanton AV, Beevers G, Pedrinelli R, Parker KH, Thom SA. Quantification of topological changes in retinal vascular architecture in essential and malignant hypertension. *J Hypertens* 2006;**24**:889–94
21. Ikram MK, Cheung CY, Lorenzi M, Klein R, Jones TLZ, Wong TYA. Retinal vascular caliber as a biomarker for diabetes microvascular complications. *Diabetes Care* 2013;**36**:750–9
22. Han H. Twisted blood vessels: symptoms, etiology and biomechanical mechanisms. *J Vasc Res* 2012;**49**:185–97
23. Annunziata R, Kheirikhah A, Aggarwal S, Hamrah P, Trucco E. A fully automated tortuosity quantification system with application to corneal nerve fibres in confocal microscopy images. *Med Image Anal* 2016;**32**:216–32
24. Lisowska A, Annunziata R, Loh GK, Karl D, Trucco E. An experimental assessment of five indices of retinal vessel tortuosity with the RET-TORT public dataset. *Annu Int Conf IEEE Eng Med Biol Soc* 2014;5414–7
25. Grisan E, Foracchia M, Ruggeri A. A novel method for the automatic grading of retinal vessel tortuosity. *IEEE Trans Med Imaging* 2008;**27**:310–9
26. Onkaew D, Turior R, Uyyanonvara B, Akinori N, Sinthanayothin C. Automatic retinal vessel tortuosity measurement using curvature of improved chain code. In: *International conference on electrical, control and computer engineering*, Kuantan Malaysia, 21–22 June 2011, pp.183–6. Piscataway, NJ: IEEE. DOI: 10.1109/INECCCE.2011.5953872
27. Ramos L, Novo J, Rouco J, Romeo S, Álvarez MD, Ortega M. Retinal vascular tortuosity assessment: inter-intra expert analysis and correlation with computational measurements. *BMC Med Res Methodol* 2018;**18**:11
28. Dougherty G, Johnson MJ, Wiers MD. Measurement of retinal vascular tortuosity and its application to retinal pathologies. *Med Biol Eng Comput* 2010;**48**:87–95
29. Cheung CY, Sabanayagam C, Law AK, Kumari N, Ting DSW, Tan G, Wong TY. Retinal vascular geometry and 6 year incidence and progression of diabetic retinopathy. *Diabetologia* 2017;**60**:1770–81
30. Jiang Y, Wang F, Gao J, Cao S. Multi-path recurrent U-Net segmentation of retinal fundus image. *Appl Sci* 2020;**10**:3777
31. Zhang TY, Suen CY. A fast parallel algorithm for thinning digital patterns. *Commun ACM* 1984;**27**:236–9
32. Ghanaei Z, Pourreza H, Banaee T. Automatic graph-based method for classification of retinal vascular bifurcations and crossovers. In: *6th international conference on computer and knowledge engineering*, Mashhad Iran, 20–21 October 2016, pp.229–34. Piscataway, NJ: IEEE. DOI: 10.1109/ICCKE.2016.7802145
33. Steacy SJ, Sammis CG. An automaton for fractal patterns of fragmentation. *Nature* 1991;**353**:250–2
34. Gadde SGK, Anegondi N, Bhanushali D, Chidambara L, Yadav NK, Khurana A, Roy AS. Quantification of vessel density in retinal optical coherence tomography angiography images using local fractal dimension. *Invest Ophthalmol Vis Sci* 2016;**57**:246–52
35. Bull SB, Mak C, Greenwood CMT. A modified score function estimator for multinomial logistic regression in small samples. *Comput Stat Data An* 2002;**39**:57–74
36. Kyurkchiev N, Markov S. On the Hausdorff distance between the heaviside step function and Verhulst logistic function. *J Math Chem* 2016;**54**:109–19
37. Khansari MM, O'Neill W, Lim J, Shahidi M. Method for quantitative assessment of retinal vessel tortuosity in optical coherence tomography angiography applied to sickle cell retinopathy. *Biomed Opt Express* 2017;**8**:3796–806
38. Fawcett T. An introduction to ROC analysis. *Pattern Recogn Lett* 2006;**27**:861–74
39. Campbell JP, Ataer-Cansizoglu E, Bolon-Canedo V, Bozkurt A, Erdogmus D, Kalpathy-Cramer J, Chiang MF. Expert diagnosis of plus disease in retinopathy of prematurity from computer-based image analysis. *JAMA Ophthalmol* 2016;**134**:651–7
40. Gelman R, Martinez-Perez ME, Vanderveen DK, Moskowitz A, Fulton AB. Diagnosis of plus disease in retinopathy of prematurity using retinal image multiscale analysis. *Invest Ophthalmol Vis Sci* 2005;**46**:4734–8

(Received March 31, 2021, Accepted June 28, 2021)